A Probabilistic Framework for Effective Wall Width Estimation in Wire Arc Additive Manufacturing

Tasbirul Alam Zihan
School of Industrial and Systems Engineering, University of Oklahoma

Abstract

Wire Arc Additive Manufacturing (WAAM) is a layer-by-layer metal additive manufacturing process that uses wire feedstock and an electric arc to build metallic components. Accurate estimation of Effective Wall Width (EWW) is important for dimensional consistency and structural integrity. This work contributes a probabilistic uncertainty-quantification framework for estimating EWW in WAAM under uncertain process inputs. The framework combines literature-based thermophysical and geometric relations to express EWW as a function of key process parameters, including heat input, wire feed speed, travel speed, and wire cross-sectional area. For Ti-6Al-4V deposition, the uncertain inputs were modeled as independent Gaussian random variables with a coefficient of variation of 15%. Monte Carlo Simulation was first used to propagate input uncertainty, while the unknown layer angle (θ) was estimated for each sample using a nonlinear solver. A lognormal distribution was then fitted to the resulting θ values and incorporated into the computational framework. To improve estimation efficiency, numerical optimization was used to identify the most probable input region contributing to EWW, and Importance Sampling was subsequently applied for variance-reduced estimation. Failure probability was estimated using quantile-based thresholding of the simulated EWW values. Overall, the study establishes a computational foundation for uncertainty-aware assessment of WAAM geometry and provides a basis for future data-informed refinement and validation.

Keywords: WAAM, additive manufacturing, uncertainty quantification, Monte Carlo simulation

1 Introduction

Additive manufacturing (AM) is a fabrication approach that constructs components layer by layer by selectively melting or fusing feedstock material, commonly in the form of wire or powder, using a heat source. The deposited material solidifies along a digitally defined trajectory, which fundamentally distinguishes additive manufacturing from conventional subtractive manufacturing techniques Herzog et al. [2016]. Compared with conventional manufacturing methods, metal additive manufacturing (MAM) offers enhanced design flexibility and reduced environmental impact, enabling the production of complex and customized geometries with lower material waste Vafadar et al. [2021]. One important MAM process is Wire Arc Additive Manufacturing (WAAM), which uses an electric arc as the heat source and metal wire as the feedstock for layer-by-layer deposition. WAAM belongs to the broader family of Directed Energy Deposition (DED) processes, which also includes techniques such as laser cladding Derekar [2018].

In the fabrication of WAAM components, two key geometric characteristics that must be controlled are the effective wall width and the layer height. These dimensions arise from the behavior of the weld pool, similar to weld reinforcement in conventional welding. In the WAAM process, the Effective Wall Width (EWW) refers to the actual physical width of the deposited wall resulting

from the interaction of process conditions. Unlike the nominal width prescribed by the toolpath, the EWW reflects the final geometric outcome and therefore serves as an important measure of dimensional accuracy and process performance. The EWW is influenced by the combined effects of arc power, travel speed, wire feed rate, inter-pass temperature, and the thermophysical properties of the material Ríos et al. [2018].

In welding-based process modeling, weld pool dimensions can be estimated from the temperature distribution within a semi-infinite solid subjected to a moving point heat source. Analytical formulations for this thermal field were originally developed by Rosenthal [1941] and Rykalin et al. [1947]. These models simplify the thermal problem by neglecting phase transformations and assuming constant thermophysical properties, which enables closed-form solutions for estimating thermal influence and resulting melt pool geometry. Later, Wells [1952] extended the analytical model of Rosenthal [1941] to relate the required weld power to the observed dimensions of the weld pool. Among the resulting formulations, this study adopts the simplified version because it provides a practical way to relate thermal input to geometric characteristics in the welding process.

The primary objective of this study is to develop a probabilistic framework for estimating EWW under uncertain process inputs using computational methods. By integrating thermal-geometric analytical models with uncertainty quantification tools such as Monte Carlo Simulation (MCS), numerical optimization, and Importance Sampling (IS), this study aims to quantify the expected value, variability, and failure probability of EWW. The main contribution of this work is a probabilistic uncertainty-quantification framework for estimating Effective Wall Width (EWW) in WAAM under uncertain process inputs. Rather than proposing a fully validated predictive process model, this study integrates literature-based thermal-geometric analytical relations with Monte Carlo Simulation, nonlinear solution of the layer angle θ, and Importance Sampling to estimate the mean, variability, and failure probability of EWW. This framework provides a computational foundation for uncertainty-aware geometric assessment in WAAM and can support future data-informed refinement and validation.

The remainder of this paper is organized as follows. Section 2 presents the theoretical background, including key probabilistic concepts such as Monte Carlo Simulation, distribution modeling, and Importance Sampling, together with the assumptions adopted in the analysis. Section 3 describes the computational methodology, including the use of MATLAB-based numerical solvers and optimization techniques for estimating uncertain geometric outputs. Section 4 presents the results and analysis, including graphical summaries, descriptive statistics, convergence behavior, failure probability estimation, and discussion of the findings in a broader engineering context. Finally, Section 5 concludes the study by summarizing the main findings and suggesting directions for future work.

2 Theoretical Background

This section outlines the fundamental probabilistic and statistical concepts that form the theoretical basis for uncertainty quantification and reliability analysis in this study. These include Monte Carlo Simulation, probability distribution modeling, Importance Sampling, and numerical optimization.

2.1 Monte Carlo Simulation (MCS)

Monte Carlo Simulation is a computational technique used to approximate expectations, integrals, and probabilities by random sampling. Given a random variable X with probability density function

List of symbols

γ	Surface tension of the molten pool	θ	Layer angle
T_m	Melting temperature of the material	TS	Travel speed of the torch
n	Empirical slope relating γ to T_m	r	Effective deposition radius
c	Intercept constant in the γ model	EWW	Effective wall width
WFS	Wire feed speed	T_0	Inter-pass temperature
A	Cross-sectional area of the wire	$\dot{Q}$	Net power into the material
ρ	Density of the material	k	Thermal conductivity
g	Acceleration due to gravity	α	Thermal diffusivity

(pdf) $p(x)$ and a function $g(x)$, the expected value of $g(X)$ is defined as:

$$E[g(X)] = \int g(x)p(x)\,dx \tag{1}$$

In MCS, this expectation is estimated empirically by drawing N independent and identically distributed samples $x_1, x_2, \ldots, x_N \sim p_x$, and computing:

$$\hat{\mu}_N = \frac{1}{N}\sum_{i=1}^{N} g(x_i) \tag{2}$$

By the **Law of Large Numbers**, $\hat{\mu}_N \to E[g(X)]$ as $N \to \infty$, and the **Central Limit Theorem** ensures that the error converges approximately as $\mathcal{N}(0, \sigma^2/N)$ for large N, where σ^2 is the variance of $g(X)$.

2.2 Probability Distributions

In this study, two key families of distributions are used:

2.2.1 Gaussian Distribution

A continuous distribution defined by mean μ and standard deviation σ, with pdf:

$$f(x) = \frac{1}{\sqrt{2\pi\sigma^2}} \exp\left(-\frac{(x-\mu)^2}{2\sigma^2}\right) \tag{3}$$

Gaussian distributions were used to model uncertainty in input parameters (e.g., heat input, WFS, TS) under the assumption that process variations are symmetric and centered around nominal values.

2.2.2 Lognormal Distribution

If a variable Y is normally distributed, then $X = \exp(Y)$ follows a lognormal distribution. The pdf of a lognormal variable is:

$$f(x;\mu,\sigma) = \frac{1}{x\sigma\sqrt{2\pi}} \exp\left(-\frac{(\ln x - \mu)^2}{2\sigma^2}\right), \quad x > 0 \tag{4}$$

2.3 Importance Sampling (IS)

Importance Sampling is a variance reduction technique used in probabilistic estimation, especially for rare event simulation or improving efficiency in Monte Carlo integration. Instead of sampling from the original pdf $p(x)$, IS samples from a proposal distribution, chosen to emphasize regions where the integrand $g(x)$ is large. The expectation is rewritten using a likelihood ratio:

$$E[g(X)] = \int g(x)p(x)\,dx = \int g(x)\frac{p(x)}{q(x)}q(x)\,dx \approx \frac{1}{N}\sum_{i=1}^{N} g(x_i)\frac{p(x_i)}{q(x_i)} \tag{5}$$

where $x_i \sim q(x)$. The weight

$$w(x_i) = \frac{p(x_i)}{q(x_i)}$$

compensates for the change in distribution. IS is particularly effective when $q(x)$ is centered around the mode or most likely region of the integrand.

2.4 Numerical Optimization

Numerical optimization techniques are employed to find points that maximize or minimize a given function. In this study, MATLAB's `fminunc` is used to maximize the integrand of the probabilistic expectation ($EWW \times$ pdf). The optimization is conducted in standard normal space, and the optimal point helps define the mean of the proposal distribution for Importance Sampling. This approach is conceptually similar to identifying a design point in reliability, though applied here in the context of integrand maximization for IS.

2.5 Failure Probability and Outlier Detection

Failure probability in this study is estimated using a non-parametric thresholding approach based on interquartile range (IQR). For dataset X, the first quartile Q_1, third quartile Q_3, and IQR are defined as:

$$IQR = Q_3 - Q_1 \tag{6}$$

Outliers are identified as samples satisfying:

$$X < Q_1 - 3 \cdot IQR \qquad \text{or} \qquad X > Q_3 + 3 \cdot IQR \tag{7}$$

These extreme values are considered as failures, and the empirical failure probability is computed as the proportion of such values.

2.6 Assumptions and Parameter Choices

To enable computational modeling, the following assumptions are made:

- All input process parameters ($\dot{Q}, WFS, TS, A$) are modeled as independent Gaussian variables.
- The coefficient of variation (CV) for each uncertain input is assumed to be 15%, reflecting moderate process variability.
- The geometric angle θ is assumed to follow a lognormal distribution, based on empirical fitting.

- All the assumed parameter values and distributions (if applicable) are provided in Tables 1 and 2.
- The residual formulation assumes quasi-steady-state energy balance and neglects convection effects within the melt pool.

2.7 Analytical models

The five analytical expressions used in this study serve to model the geometric and thermal behavior of WAAM-deposited layers. Equation (1), constructed from the work of Aune et al. (2005), provides a linear relationship between the surface tension γ of the molten pool and the melting temperature T_m, governed by an empirical slope n and intercept c. The rest of the equations are adapted from Ríos et al. (2018). Equation (2) expresses the melt pool temperature T_m as a function of deposition process parameters including wire feed speed (WFS), cross-sectional area of the wire (A), material density ρ, gravitational acceleration g, travel speed (TS), and the layer angle θ, incorporating the effect of geometric orientation through trigonometric terms.

Table 1: Parameters with uncertain values

Parameter	**Mean value**	**Unit**	**Source**
$\dot{Q}$	734	W	Ríos et al. (2018)
TS	2	mm/s	Ríos et al. (2018)
WFS	1.2	m/min	Ríos et al. (2018)
A	0.7854	mm^2	Ríos et al. (2018)

Table 2: Parameters with constant values

Parameter	**Value**	**Unit**	**Source**
n	-0.00058065	–	Aune et al. (2005)
c	2.32	–	Aune et al. (2005)
ρ	4430	kg/m^3	–
g	9.8	$m\,s^{-2}$	–
T_0	373	K	Ríos et al. (2018)
k	24	$Wm^{-1}K^{-1}$	Ríos et al. (2018)
α	7.79×10^{-6}	$m^2\,s^{-1}$	Ríos et al. (2018)

$$\gamma = n \cdot T_m + c \tag{8}$$

$$T_m = \frac{WFS \cdot A \cdot \rho \cdot g \cdot \left(1 + \sin\left(\frac{\theta}{2}\right)\right)}{n \cdot TS \cdot (\theta + \sin\theta)} - \frac{c}{n} \tag{9}$$

Equation (3) defines the effective deposition radius r as a function of the same deposition parameters, quantifying how far the molten metal spreads laterally from the center of the bead. Equation (4) calculates the effective wall width (EWW) as a geometric projection of the deposition radius r, adjusted for the layer angle θ, thereby capturing the actual horizontal contribution of a single deposited layer. Finally, Equation (5) models the thermal energy balance by equating the net energy input $\dot{Q}$ to the rise in temperature from a baseline inter-pass temperature T_0 to the melt temperature T_m, accounting for thermal conductivity k and thermal diffusivity α. These five

expressions collectively form the foundation for the probabilistic estimation framework used in this work.

$$r = \sqrt{\frac{WFS \cdot A}{TS \cdot (\theta + \sin\theta)}} \tag{10}$$

$$EWW = 2r \cdot \cos\left(\frac{\theta}{2}\right) \tag{11}$$

$$T_m - T_0 = \frac{\dot{Q}}{4k \cdot EWW}\left(0.2 + r\left(\sin\left(\frac{\theta}{2}\right) + \frac{\pi}{4}\right) \cdot \frac{TS}{2\alpha}\right)^{-1} \tag{12}$$

3 Methodology

3.1 Computational Approach

The core computational methods employed in this study are Monte Carlo Simulation (MCS) and Importance Sampling (IS). These techniques were chosen to address the probabilistic nature of input uncertainties and their propagation through nonlinear analytical models governing the WAAM process.

Monte Carlo Simulation was first used to quantify the uncertainty in the geometric parameter θ, which influences the EWW. Random samples for uncertain process parameters WFS, TS, A, and $\dot{Q}$ were drawn from Gaussian distributions with a coefficient of variation (CV) of 15%. For each random set of inputs, a nonlinear equation was solved numerically using a root-finding algorithm (`fsolve` in MATLAB) to compute the corresponding value of θ.

To improve the efficiency and accuracy of EWW estimation, Importance Sampling was employed. A local maximum of the integrand (EWW weighted by a Gaussian density function) was identified using unconstrained optimization (`fminunc` in MATLAB), and the optimal point was used to define a new proposal density. This IS-based sampling is adopted to calculate the expected value of EWW with lower variance compared to plain MCS.

The expected value of EWW was then computed as a weighted mean, and a coefficient of variation was calculated to assess convergence and estimation reliability. Lastly, failure probability was estimated using a quantile-based thresholding approach on the EWW samples.

All computational steps were implemented in MATLAB, chosen for its robust support for numerical solvers (`fsolve`, `fminunc`), statistical functions (`mvnrnd`, `mvnpdf`), and matrix-based vectorized operations that are well-suited for high-volume stochastic simulations.

3.2 Implementation

The computational methods described were implemented entirely in **MATLAB**, using a structured workflow divided into five main stages: model definition, nonlinear solving, parameter optimization, EWW estimation, and failure probability estimation. The corresponding flowchart summarizing the entire implementation process is presented in Figure 1.

3.2.1 Analytical Model Definition

All five governing equations for the WAAM process were implemented as MATLAB functions. These included expressions for melt-pool temperature T_m, effective deposition radius r, and Effective Wall Width (EWW), as well as the thermal balance equation used to solve for θ. The residual

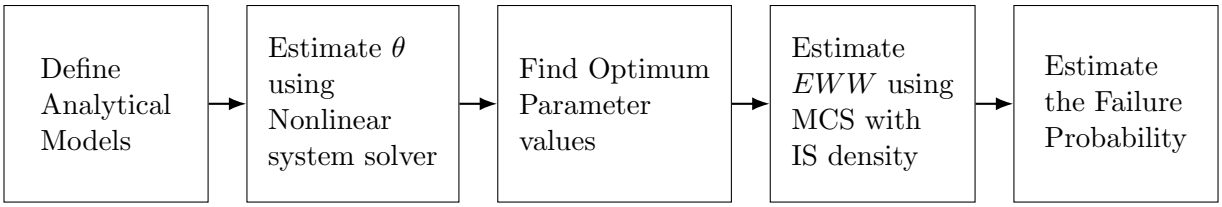

Figure 1: Workflow of the methodology

for the nonlinear equation was encapsulated in a well-defined function, which took the five input parameters and returned the squared error between the LHS and RHS of the thermal equation.

3.2.2 Estimating θ via Monte Carlo Simulation

To account for uncertainty in the input parameters $\dot{Q}$, WFS, TS, and A, 3,000 samples were generated, assuming normal distributions with 15% CV. For each sample set, the nonlinear system was solved using `fsolve` to obtain a corresponding value of θ. The resulting θ values were then used to estimate a lognormal distribution that best fit the empirical data.

3.2.3 Finding Optimal Parameters via Local Maximum

To improve sampling efficiency, the integrand representing the product of EWW and the standard normal PDF, which is shown in Equation (13), was maximized using `fminunc`. This step returned the optimal point x^{g*} in standard Gaussian space, which was transformed back into physical space and found point x^* for using in Importance Sampling.

$$E[EWW] = \int EWW(x)\, f(x)\, dx \tag{13}$$

$$x^* = \begin{bmatrix} \dot{Q}^* \\ TS^* \\ WFS^* \\ A^* \\ \theta^* \end{bmatrix}$$

3.2.4 Estimating EWW Using Importance Sampling

Using the optimized point, 3,000 samples were generated from a gaussian proposal distribution centered at x^{g*}, and each was transformed back to physical space. For every sample, EWW was computed using the analytical expressions. The expected value of EWW was estimated using IS-weighted averages, as mentioned in Equation (14), and convergence was assessed using the coefficient of variation, as presented in Equation (15).

$$E[EWW] = \text{mean}_{\{x^{q,j}\}_{j=1,\ldots,K}} \left(EWW(x^{q,j}) \frac{f^g(x^{q,j})}{q^g(x^{q,j})} \right) \tag{14}$$

$$\delta_{IS,K} \approx \frac{1}{\sqrt{K}} \frac{\sqrt{\text{variance}_{\{x^{q,j}\}_{j=1,\ldots,K}} \left(EWW(x^{q,j}) \frac{f^g(x^{q,j})}{q^g(x^{q,j})} \right)}}{\text{mean}_{\{x^{q,j}\}_{j=1,\ldots,K}} \left(EWW(x^{q,j}) \frac{f^g(x^{q,j})}{q^g(x^{q,j})} \right)} \tag{15}$$

3.2.5 Failure Probability Estimation

A quantile-based method was applied to determine failure thresholds. The interquartile range (IQR) of the EWW estimates was used to define upper bounds. For Q_1 and Q_3 being the first and third quartiles, any EWW falling outside the range $[Q_1 - 3 \cdot IQR,\ Q_3 + 3 \cdot IQR]$ was classified as a failure. The final failure probability was computed as the ratio of the number of failures to total samples.

4 Results

The results obtained from the computational workflow are presented and interpreted in this section. The focus is on analyzing the behavior of the estimated parameters, the accuracy of the Effective Wall Width (EWW) estimation, convergence of the simulation, and the computed failure probability.

4.1 Estimation of θ

Using Monte Carlo Simulation (MCS) and nonlinear solving via `fsolve`, the angular parameter θ was estimated for 3,000 samples, as shown in Figure 2(a). The resulting histogram in Figure 2(b) showed a positively skewed distribution. Fitting a lognormal distribution to the samples yielded a mean of approximately 0.7645 rad ($\approx 40.83°$) and a variance of 0.4281, supporting the appropriateness of the lognormal model. The fitted distribution closely aligned with the observed histogram, confirming the stability of the solver under uncertainty propagation.

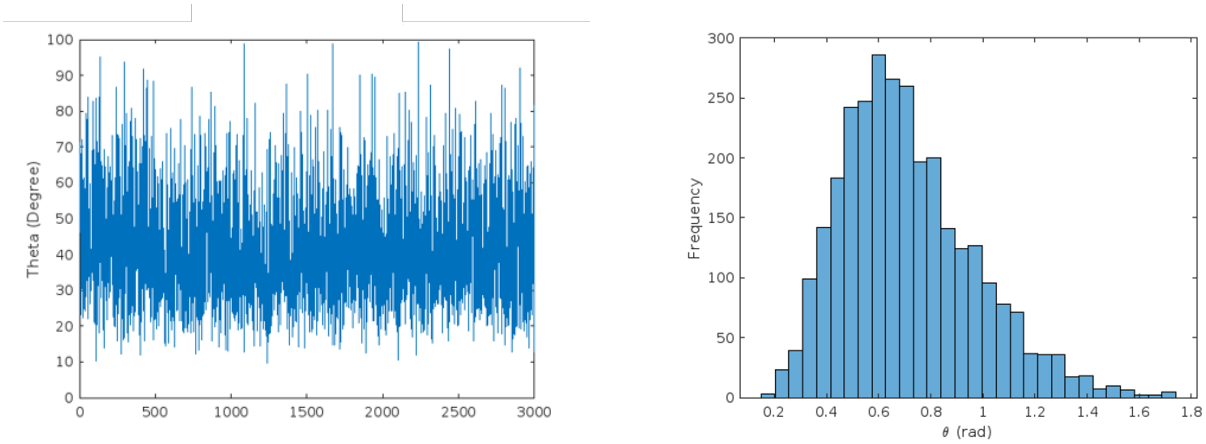

(a) (b)

Figure 2: (a) θ values for all iterations; (b) histogram of the θ values.

4.2 Optimal Parameter Estimation

To support efficient importance sampling, the integrand of the probabilistic model was maximized. The optimal values for the five uncertain parameters $\dot{Q}$, TS, WFS, A, and θ were obtained via numerical optimization (`fminunc`) and transformed back into physical space. The optimal values are:

$$x^* = \begin{bmatrix} \dot{Q}^* \\ TS^* \\ WFS^* \\ A^* \\ \theta^* \end{bmatrix} = \begin{bmatrix} 734 \text{ W} \\ 0.002 \text{ m s}^{-1} \\ 0.0203 \text{ m s}^{-1} \\ 7.97 \times 10^{-7} \text{ m}^2 \\ 1.00 \text{ rad} \end{bmatrix}$$

These values ensured higher probability density near the region contributing most to the EWW integral, enhancing accuracy.

4.3 EWW Estimation Using Importance Sampling

With the optimized parameters as the mean of the proposal distribution, 3,000 samples were generated and used to compute EWW using the analytical expression. The expected value of EWW was found to be 0.0015 m. The coefficient of variation (CV) was tracked as a function of sample count and converged smoothly to 2.93%, indicating a stable and reliable estimator. Convergence of both the expected values and the coefficient of variation is shown in Figure 3. This low CV validates the accuracy and efficiency of the importance sampling approach used in the simulation.

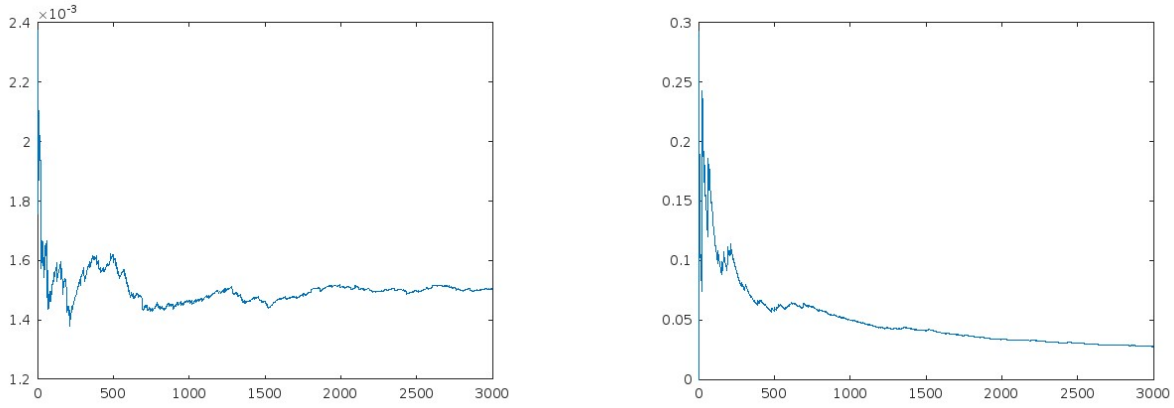

(a) (b)

Figure 3: (a) Convergence of estimated EWW to a stable value; (b) convergence of CV toward 0.

4.4 Failure Probability Estimation

Using the quartile thresholding method, the first quartile, $Q_1 = 0.0015$, and third quartile, $Q_3 = 0.0025$, of the EWW estimates were calculated, and an interquartile range (IQR) was used to define the failure region. EWW values outside the bounds $[Q_1 - 3 \cdot IQR,\ Q_3 + 3 \cdot IQR]$ were considered failures. The final failure probability $P(F)$ was computed as 0.0753 or 7.53%, indicating a relatively low chance of geometrical non-conformance under the assumed input uncertainty (15% CV).

4.5 Discussion

The computational study provides a probabilistic framework to estimate the effective wall width (EWW) in wire arc additive manufacturing (WAAM), incorporating input uncertainties and quantifying the likelihood of geometrical failure. The findings reinforce the critical role of stochastic modeling in capturing the variability inherent to WAAM processes and highlight how Monte Carlo

based techniques, especially importance sampling (IS), can enhance the efficiency and accuracy of such estimations.

The successful fit of a lognormal distribution to the Monte Carlo sampled values of the layer angle θ was consistent with expectations, as angular variability in deposition processes typically exhibits asymmetric, right-skewed behavior with positive values. This provided a more realistic input for downstream geometric calculations and improved the relevance of the simulation results.

One of the key insights from the results is the relatively low coefficient of variation (CV $\approx 2.93\%$) in the EWW estimates when using importance sampling, despite the initial assumption of 15% CV for all five uncertain input variables. This indicates that the EWW is not highly sensitive to simultaneous moderate variations in the considered parameters or, more precisely, that the IS approach effectively concentrates sampling in the high-contribution region of the integrand, thereby reducing estimator variance.

Theoretically, based on experimental findings reported in Ríos et al. [2018], the expected range of Effective Wall Width (EWW) for cylindrical Ti-6Al-4V WAAM deposits typically falls between 5 to 10 mm. However, the computational results in this work consistently converged to an average EWW of approximately 1.5 mm in the Monte Carlo Importance Sampling simulation. This significant divergence suggests that either the assumed parameter distributions or the simplifying assumptions in the analytical models may not fully reflect realistic industrial conditions. It may also indicate that the use of a highly conservative angle θ distribution (lognormal with limited spread) restricted the geometric output range. Hence, while the computational framework demonstrates good numerical convergence and internal consistency, its predictive fidelity relative to physical expectations is limited by the idealized input assumptions and model structure. This highlights the need for real process data and more accurate parameter assumptions in future refinements.

The estimated failure probability of 7.53% based on quartile based thresholding provides an interpretable and application-agnostic measure of process reliability. However, this measure is inherently statistical and lacks physical or application-specific failure definitions. In practice, the notion of failure would be tied to tolerances based on functional or structural requirements of the printed parts, which this model does not capture.

There are several assumptions that could affect the generalizability of the results. Firstly, all uncertain input parameters were modeled as Gaussian with 15% CV, which may not reflect real process distributions, particularly for physical parameters like heat input or inter-pass temperature. Secondly, the analytical equations used, especially the simplified form of Rosenthal's heat transfer model and empirical correlations from literature, do not capture complex thermophysical phenomena such as phase transformations, temperature-dependent material properties, or dynamic torch movement effects. These simplifications, while necessary for analytical tractability, may limit the model's accuracy in capturing real-world deviations.

Moreover, the analysis focused on a single material, Ti-6Al-4V, and fixed process parameter ranges derived from prior literature. Any deviation in material behavior or process window would require recalibration of the statistical assumptions.

In a broader context, this work illustrates the potential for using computational probability and stochastic optimization in additive manufacturing design and control. The framework is adaptable and can be extended to other geometric metrics (e.g., layer height) or defect-related properties with appropriate modifications to the governing equations and sampling strategies.

5 Conclusion

This study presented a probabilistic uncertainty-quantification framework for estimating and analyzing the effective wall width (EWW) in wire arc additive manufacturing (WAAM) of Ti-6Al-4V under uncertain process parameters. Rather than proposing a fully validated predictive process model, the study developed a computational framework that combines analytical thermal-geometric relations, Monte Carlo Simulation (MCS), nonlinear estimation of the layer angle θ, and Importance Sampling (IS) to quantify the expected value, variability, and failure probability of EWW. The analytical expressions adopted from prior literature were used to relate thermal and geometric quantities to the final deposition shape, while stochastic simulation was employed to propagate uncertainty through the model.

The computational results demonstrated good numerical convergence and stability across both MCS and IS implementations. However, the average EWW estimated from the simulations (~ 1.5 mm) was significantly lower than typical experimental values (5–10 mm), highlighting a discrepancy between the theoretical model assumptions and real-world process behavior. This result emphasizes the importance of improving input accuracy using empirical data and refining the modeling assumptions used in the computational framework.

Future work should focus on incorporating real sensor-driven process data to better characterize parameter distributions and improve model realism. In addition, more advanced surrogate modeling or Bayesian inference frameworks could be used to quantify correlations among inputs and update the model as new observations become available. Overall, this work provides a computational foundation for uncertainty-aware geometric assessment in WAAM and offers a pathway toward more reliable quality prediction and control under uncertainty.

References

KS Derekar. A review of wire arc additive manufacturing and advances in wire arc additive manufacturing of aluminium. *Materials science and technology*, 34(8):895–916, 2018.

Dirk Herzog, Vanessa Seyda, Eric Wycisk, and Claus Emmelmann. Additive manufacturing of metals. *Acta Materialia*, 117:371–392, 2016.

Sergio Ríos, Paul A Colegrove, Filomeno Martina, and Stewart W Williams. Analytical process model for wire+ arc additive manufacturing. *Additive Manufacturing*, 21:651–657, 2018.

Daniel Rosenthal. Mathematical theory of heat distribution during welding and cutting. *Welding journal*, 20(5):220s–234s, 1941.

NN Rykalin et al. Thermal fundamentals of welding. *USSR Academy of Sciences, Moscow-Leningrad*, 1947.

Ana Vafadar, Ferdinando Guzzomi, Alexander Rassau, and Kevin Hayward. Advances in metal additive manufacturing: a review of common processes, industrial applications, and current challenges. *Applied Sciences*, 11(3):1213, 2021.

AA Wells. Heat flow in welding. *JAWS*, 31:263, 1952.